

Enumeration of illumination and scanning modes from real-time spatial light modulators

Li Ge, Markus Duelli and Robert W. Cohn

*ElectroOptics Research Institute, University of Louisville
Louisville, KY 40292 USA
rwohn@louisville.edu*

Abstract: Using a phase-only spatial light modulator (SLM) in a Fourier transform setup together with fast diffractive optics design algorithms provides a way to automatically generate complex and rapidly changing laser illumination patterns in the far-field. We propose a hierarchical software structure for the adaptive, on-line design of far-field illumination patterns. Using the on-line design system together with camera feedback of the illuminated scene would make it possible to detect and actively laser designate multiple objects in parallel. Possibilities for multispot, arbitrary trajectory scanning and also broad-area speckle-reduced illumination are demonstrated with experimentally measured diffraction pattern sequences from a 120 x 128 pixel phase-only SLM.

© 2000 Optical Society of America

OCIS codes: (070.2580) Fourier optics; (230.6120) spatial light modulators; (090.1760) computer holography; (090.1970) diffractive optics; (030.6600) statistical optics

References and links

1. U. Krackhardt, J.N. Mait, and N. Streibl, "Upper bound on the diffraction efficiency of phase-only fanout elements," *Appl. Opt.* **31**, 27-37 (1992).
2. R. W. Cohn and L. G. Hassebrook, "Representations of fully complex functions on real-time spatial light modulators," Ch. 15, pp. 396-432 in *Optical information processing*, F. T. S. Yu and S. Jutamulia, eds. (Cambridge U. Press., Cambridge, UK, 1998).
3. Galvanometer scanners and accessories, http://www.gsilumonics.com/c03oem_gal_frame/galvoframe.html
4. Cambridge Technology Products, <http://www.camtech.com/prods4a.htm>
5. NEOS online catalog, <http://www.neostech.com/neos/catalog>
6. Isomet Corporation deflectors, <http://www.isomet.com/deflectors.html>
7. Boulder Nonlinear Systems, Inc., <http://www.bnonlinear.com>
8. T. H. Lin, "Implementation and characterization of a flexure-beam micromechanical spatial light modulator," *Opt. Eng.* **33**, 3643-3648 (1994).
9. M. Duelli, M. Reece, and R. W. Cohn, "Modified minimum distance criterion for blended random and nonrandom encoding," *J. Opt. Soc. Am. A* **16**, 2425-2438 (1999).
10. M. Duelli, R. W. Cohn, "Pseudorandom encoding for real-valued ternary spatial light modulators," *Appl. Opt.* **38**, 3804-3809 (1999).
11. L. Ge, M. Duelli, and R. W. Cohn, "Improved-fidelity error diffusion through blending with pseudorandom encoding," *J. Opt. Soc. Am. A* **17**, 1606-1616(2000).
12. R. W. Cohn and M. Liang, "Approximating fully complex spatial modulation with pseudo-random phase-only modulation," *Appl. Opt.* **33**, 4406-4415 (1994).
13. R. W. Cohn and M. Duelli, "Ternary pseudorandom encoding of Fourier transform holograms," *J. Opt. Soc. Am. A* **16**, 71-84 and "errata," 1089-1090 (1999).
14. R. D. Juday, "Optimal realizable filters and the minimum Euclidean distance principle," *Appl. Opt.* **32**, 5100-5111 (1993).
15. Y. Yang, H. Stark, D. Gurken, C. L. Lawson, and R. W. Cohn, "High-diffraction-efficiency pseudorandom encoding," *J. Opt. Soc. Am. A* **17**, 285-293 (2000).
16. J. N. Mait, "Understanding diffractive optic design in the scalar domain," *J. Opt. Soc. Am. A* **12**, 2145-2158 (1995).
17. D. Jared and D. Ennis, "Inclusion of filter modulation in synthetic discriminant function construction," *Appl. Opt.* **28**, 232-239 (1989).
18. N.C. Gallagher and B. Liu, "Method for computing kinoforms that reduces image reconstruction error," *Appl. Opt.* **12**, 2328-2335 (1973).
19. R. W. Cohn, "Adaptive real-time architectures for phase-only correlation," *Appl. Opt.* **32**, 718-725 (1993).
20. M. S. Vangular, *Optimization methods for diffraction gratings and composite matched filters*, M.S. Thesis,

1. Introduction

Spatial light modulators (SLM) can be used both as image displays and as programmable real-time diffractive optical elements (DOE). The second application is the area addressed by this paper. Programmable diffraction has a decided advantage over image display when the image consists of only a few bright pixels. Consider that when an SLM of N pixels is imaged, only $\sim 1/N$ of the energy in the SLM aperture is found in one pixel of the image. However, when laser light is diffracted, as much as 100% of the light in the aperture (ignoring practical sources of loss; e.g., sampling effects and absorption) can be diffracted into a single pixel (specifically, a diffraction-limited spot.) Also, specially designed and optimized DOE's have been demonstrated that diffract the incident energy into 10-1000 equal intensity spots with efficiencies of 90 % to 100 % [1]. For SLM's that contain from 128^2 to 512^2 pixels it can be seen that for patterns of 1000 spots the SLM pattern can be $\sim 16X$ to $250X$ brighter when used as a programmable DOE than when used as an image display.

This result suggests roles for diffractive SLM's in multi-spot scanning and scene illumination that are more general than traditional single-spot mechanical (and also acousto-optic) scanners. Unlike traditional scanners, frame-addressed SLM's are non-inertial and have no memory (as long as the modulating material response time is shorter than the SLM framing time.) Since frame-addressed SLM's can produce sequences of unrelated images, the sequences can be designed that scan multiple spots on arbitrary trajectories and with different velocities and intensities. Because these possibilities are unlike those for previous scanning systems, the goal of this paper is to describe the physical differences between traditional, inertial type scanners and diffractive SLM based illuminators (Section 2), to present the software programming and computational considerations for on line design of the required SLM modulation patterns (Section 3), and to experimentally demonstrate, using a phase-only SLM, some of the generalized scanning and illumination functions that are possible using diffractive, frame-addressed SLM's (Section 4).

While the diffraction patterns that we will present are generated at real-time rates, the SLM modulation patterns usually were designed and optimized off-line. A continuing goal in our research is to develop an attached computer/hardware/software system that automatically designs the modulation patterns at real-time rates [2]. We recognize that any practical system developed will require a tradeoff between optical performance and computational load. This leads to us proposing in Section 3 a three-level, hierarchical design strategy that trades off optical performance versus available computation time. We believe that for many applications it will be reasonable to design patterns automatically at real-time rates and with sufficient optical quality to permit laser designation of multiple moving objects. Herein we describe a proposed multi-spot scanning system in enough detail to permit evaluation of the new functionality provided together with a description of system design considerations and fundamental limitations.

2. Distinctions between inertial scanners and frame-addressed SLM's for scanning

Inertial scanners include galvanometers and acousto-optic Bragg deflectors. These devices have the ability both to point or to continuously scan a laser beam. Even when producing spots at non-sequential locations the beam usually is scanned continuously, which may require the laser to be shuttered if the line between two points is not to be illuminated. Ideally frame-addressed SLM's produce sequential images and shuttering of the laser source is not required. However, stray light can be generated during the transition time between successive SLM frames due to the finite response time of the modulating material. When the SLM framing time is close to the material response time, the energy in stray light can be comparable to the energy in the desired pattern.

Thus at limiting frame rates, shuttering of the laser may be necessary.

While inertial scanners can produce continuous line scan automatically, frame-addressed SLM's cannot. Furthermore the time required to scan a line over the full angular range of the device is of the same order as the time to repoint the laser to an arbitrary position. To approximate a continuous scan line with SLM's the diffraction patterns must sample space without leaving any gaps. This problem corresponds to successively sampling the diffraction plane n times with a diffraction limited spot, where n is the number of pixels in a $n \times n$ pixel SLM. If the frame rate of the SLM is identical to the frequency of the inertial scanner then the inertial scanner is n times faster than the SLM.

However, this is a worst case comparison which does not take into account the additional capabilities of SLM's to produce multiple spots in parallel and to produce illumination patterns with footprints that are larger than the diffraction limit. The difference in scan speeds between inertial and SLM scanning can be reduced to n/m_1 by using the SLM to scan m_1 diffraction limited spots along the scan direction, or by broadening/blurring a spot by a factor of m_2 which leads to a speed comparison of n/m_2 . Also varying combinations of scanning and blurring can be used to obtain a speed comparison of $n/(m_1 m_2)$. (Note: This speed comparison is not meant to reflect that both blurring and multiple spots increase scanning more than either does individually. Instead the speed comparison suggests that various combinations of blurring and multiple spots can be used to scan continuously with a SLM.)

Examples of these possibilities either have been presented previously or are presented herein. In Section 4 we present an example of scanning an array of multiple spots. One way to obtain blurring of the spots is to partition the SLM into sub-arrays in which the aperture of each sub-array sets the diffraction limited spot size. Another way is to design an effective apodization into the modulation pattern that blurs or broadens the spots.

We complete this comparison by considering the speeds of various devices. Commercial galvanometric scanners scan at rates up to their resonant frequency ~ 5 kHz and take small steps at ~ 0.2 ms [3,4]. Acousto-optic Bragg deflectors can scan in excess of 1 MHz [5,6]. The speeds of the galvanometers are comparable to the frame rate of current liquid crystal on silicon SLM's (10 kHz for the BNS 128 x 128 pixel SLM) [7]. However, for analog phase modulation over a full 2π range nematic liquid crystal is used. Its response time is ~ 2 to 4 ms which would limit useful frame rates to ~ 250 Hz. Even at this low rate a single diffraction-limited spot (and also multiple spots) could be continuously scanned over the 128 resolution cells 2 times per second. A faster phase shifting device that is not commercially available at this time is the flexure beam deformable mirror device. Response times of under $10 \mu\text{s}$ have been reported [8]. Given fast enough frame addressing circuits then ~ 800 scans per second per spot or faster is possible. Using the frame rate of the BNS addressing circuit as a reasonably practical number gives ~ 80 scans per second. The SLM used for the experiments in this study is the BNS SLM described above. It is filled with nematic liquid crystal and thus is limited to practical frame rates of around 250 Hz and 2 complete line scans per spot per second.

In order to clarify the differences between frame-addressed SLM's and traditional scanners we have compared their speeds at continuous scanning of the full field of regard. By this comparison SLM's appear to be quite slow. However, the applications we envision for the SLM (while they may require an occasional full field scan) do not require repetitive full field scanning for which traditional scanners are best suited. Specifically, we envision using an SLM illuminator together with feedback from a video camera viewing the illuminated scene to adaptively track and designate objects of interest in the scene. The ability to configure patterns flexibly provides a way to intelligently interrogate the field of regard. Using information gained from previous video frames on object motion provides a way to reduce the total area of the scene that needs to be illuminated. Used in this way it appears likely that even the 250 Hz frame rate SLM reported in this study has adequate frame rate to support adaptive tracking and designation of multiple objects in situations where the motion of the objects is neither too fast nor too erratic to be predicted.

3. Hierarchical DOE design system

In addition to the physical limitations that set SLM frame rate there is also a computational limitation. For the adaptive type applications that we are considering, it usually will not be possible to predetermine an appropriate set of desired diffraction patterns. Therefore it will be necessary to design the required spatial modulations for the SLM on-line as needed.

Current methods of designing fixed pattern DOE's usually use global search and optimization to identify modulation patterns that produce the best possible diffraction patterns. These methods are computationally intensive. The reason is that there are a near infinite number of Fourier transform pairs that have identical intensity diffraction patterns but which have different phase diffraction patterns. In illuminator systems, in which only the intensity of the desired diffraction pattern is of interest, global search and optimization are used to identify the phase diffraction pattern that gives the best performing intensity diffraction pattern. If the SLM can produce any arbitrary complex value of modulation then all diffraction patterns are identical except for an intensity scale factor. The optimization algorithm searches for the modulation pattern that maximizes the intensity (and hence, the diffraction efficiency) of the diffraction pattern. However, most modulators are not fully complex, and thus the diffraction pattern may only approximate the desired diffraction pattern. Then the optimization algorithm needs to trade off diffraction efficiency with accuracy or "fidelity" of the intensity pattern.

Because optimization methods are computationally intensive, it may not be possible to complete the calculation at the frame rate required for a real-time illumination system. Faster, but lower performing, algorithms can be used to reduce computation time. Then, if additional time becomes available (e.g. there is little change in a scene for a period of time) design algorithms that produce higher performance are used. This introduces the hierarchical design strategy needed for on-line design. Fig. 1 summarizes one approach to on-line design that has three levels of computational complexity.

Level 1: Minimum Time Design. The design method starts with a specification of $I_T(f)$ the desired target intensity pattern in the diffraction plane. For a target diffraction pattern composed of an array of spots we may specify the desired $I_T(f_i)$ for the discrete set of frequencies f_i . These values together with any arbitrary set of phases ϕ_i specify the complex light distribution $\mathbf{A}_c'(f_i)$. The complex valued function $\mathbf{a}_c'(x)$ where x is the modulator plane coordinate can then be calculated (the compose function block in Fig. 1a.) Composition can be performed using the inverse fast Fourier transform (IFFT) of $\mathbf{A}_c'(f)$. However from the standpoint of ease of use or numerical efficiency it may be preferred to use known Fourier transform pairs $\mathbf{g}_i(x) \leftrightarrow \mathbf{G}_i(f)$ and $\exp(j2\pi f_i x) \leftrightarrow \delta(f-f_i)$ followed by the superposition of these elementary functions to give

$$\mathbf{a}_c'(x) = \sum_{i=1}^M \mathbf{g}_i(x) \exp[j(2\pi f_i x + \phi_i)]. \quad (1)$$

The magnitude of function $\mathbf{a}_c'(x)$ is then rescaled so that the maximum magnitude is unity (normalization step in Fig. 1a with γ initially equal to unity) which produces the normalized function $\mathbf{a}_c(x)$. The normalized function $\mathbf{a}_c(x)$ is mapped through a selected encoding algorithm into a modulation $\mathbf{a}(x)$ that is achievable with the limited modulation range of the non-fully complex SLM. The diffraction pattern intensity $I(f)$ is produced by the optical Fourier transform (OFT).

The normalization step in Fig. 1a is suggested by the fact that SLM's are passive devices. However, the actual reason for this step is that while some algorithms can be applied if magnitudes are greater than unity, many encoding algorithms cannot [2]. Furthermore, of the encoding algorithms that can handle magnitudes that are greater than unity, many of these algorithms nonetheless depend on the exact scaling of the function. (Scaling is discussed further in the next subsection on Level 2 design).

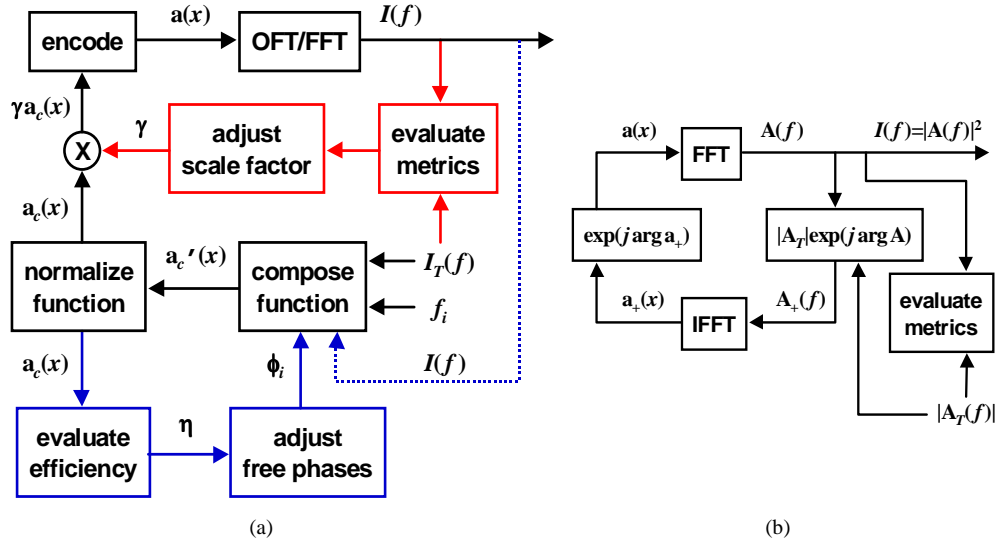


Fig. 1. (a) The proposed hierarchical design system, (b) the iterative Fourier transform algorithm. In (a) Level 1 design is indicated by black lines and boxes. With the addition of the algorithmic portions indicated by red and blue lines, the algorithm becomes a Level 2 or Level 3 design respectively. The errors between the target and resulting intensities (dashed blue line) can be used to compensate the desired function, and this procedure, which is similar to adjustment of the free phases, also is classified as Level 3 design.

The major computational time for the Level 1 design includes composing the function $a_c'(x)$ (which requires when using superposition either $O(NM)$ function calculations for an N pixel SLM and M frequencies of interest f_i , or when using IFFT $O[M \log_2(N)]$ multiplies,) and encoding [which requires $O(N)$ function calculations.] For a small enough number of diffraction spots [i.e. for $M < \alpha \log_2(N)$ where α is a scale factor accounting for the exact differences in computation time between the IFFT and superposition algorithms,] superposition of Fourier transform pairs requires less computation time. While composition of the desired function requires $O(M)$ times more calculations than encoding, the elemental functions can be synthesized in parallel which, at the cost of added (analog or digital) processing hardware, would permit the rate of function calculation to match the rate of encoding.

Level 2: Moderate Time Design. If there is additional computation time available after completing Level 1, the desired complex function can be encoded by multiple algorithms and the encoding that produces the most satisfactory diffraction pattern is selected. Example of this are the hybridization of multiple encoding algorithms [9-11]. The hybridization is characterized by one (or more) parameter(s) γ that defines which regions of the complex plane are encoded by which algorithm. For instance, in the minimum distance-pseudorandom encoding algorithm (MD-PRE) for phase-only SLM's in Ref. [9], values of the scaled function $\gamma a_c(x)$ (see Fig. 1a) with magnitudes less than unity are encoded by pseudorandom encoding algorithm (PRE) [12,13] and complex values with magnitudes greater than unity are encoded by minimum distance encoding (MDE) [14]. The best performance in terms of specific fidelity measures (e.g. non-uniformity, signal-to-peak-noise ratio) is usually found for a particular blending of MD-PRE as specified by the value of γ . We are unaware of an *a priori* method to select or estimate the best value of γ . This leads to our proposal to adjust blending parameters based on the resulting intensity pattern $I(f)$ (as indicated by the innermost feedback loop in Fig. 1a.) The intensity pattern can be simulated using the FFT, but it can be faster to use the OFT to produce a diffraction pattern and then measure its intensity with a digital camera. Since only intensity, and not phase, is needed to find the optimal value of γ , digital measurement and feedback of the diffraction pattern is reasonably practical.

Level 3: Maximum Time Design. If there is significantly more time available than required to complete Levels 1 and 2, then DOE type design, which includes multiple iterations of a global search and/or optimization method can be employed. The approach indicated in Fig. 1a is to compose and evaluate multiple functions $\mathbf{a}_c(x)$ that satisfy the target intensities $I_T(f_i)$. Generally the higher the diffraction efficiency η of the complex valued function, the more closely $I(f)$ compares to $I_T(f)$ [15].

There are many methods possible to select the phase free parameters ϕ_i (e.g. Monte Carlo selection, gradient search, genetic algorithms and projection onto constraints [15,16]) that could be used in this block of the Fig. 1a flowchart. While $\mathbf{a}_c(x)$ can be computed using the IFFT, this calculation can be avoided by superposition of known Fourier transform pairs, which can be faster, as discussed above. Methods of optimizing a complex function followed by encoding is classified by Mait as an indirect design method [16]. Mait observed that better performance is achieved for direct methods, in which the available modulation values are directly adjusted to produce the best solution, but that this may also entail a greater amount of computation than the indirect method. It is the time constraints in real-time pattern generation that suggest our indirect design strategy that is based on composition of fully complex functions followed by encoding.

One limitation of our indirect procedure is that by first selecting $\mathbf{a}_c(x)$ followed by encoding can introduce deviations between $I(f)$ and $I_T(f)$ [16]. It is possible to compensate values of resulting intensity $I(f_i)$ that are greater (less) than the target intensities $I_T(f_i)$ by reducing (increasing) the magnitude scale of the corresponding functions $\mathbf{g}_i(x)$ in eq. (1) (e.g. using the gradient method of Jared and Ennis [17].) Even with feedback of the resulting values of $I(f)$ to adjust $\mathbf{a}_c(x)$ (dashed path in Fig. 1a) this modified procedure, though it has an increased computational load is classified as an indirect design method.

Discussion: We have described a framework for on-line design of modulation patterns for SLM's used in a Fourier transform arrangement. The structure is designed to ensure that at least one realization of the desired diffraction pattern can be implemented in as short a time as possible. There are many algorithms that can be used to implement the various blocks, and we do not restrict the system to specific algorithms. Instead, we focused on the relative computation times of the major blocks in order to provide a first look at key issues limiting design time. A more detailed analysis involving numerical and digital implementations of FFT's, arithmetic and function calculations, depends on many design- and application-specific issues and is beyond the scope of this report. However, we did focus on ways in which the use of the FFT (by OFT) and IFFT (by superposition of known Fourier transform pairs) could be avoided to reduce the computation time. In contrast to Fig.1a, consider Fig. 1b which shows a typical structure used in the fixed pattern DOE design. This is the iterative Fourier transform algorithm (IFTA) [18]. Similar to Fig. 1a, the IFFT can be replaced by using superposition. The FFT in Fig. 1b could be replaced with the OFT; however, in addition to intensity, phase also must be measured, which requires more involved hardware [19] For the proposed framework in Fig. 1a, Level 1 provides the shortest path to an initial design. If even shorter design times than possible with Level 1 are required, then further customization of the design may be possible for some applications. One way is to design for only a limited subset of the N SLM pixels. Examples of this approach are presented in Section 4.

Portions of the proposed structure in Fig. 1a have been demonstrated in off line design studies. In Refs. 9, 11 respectively we have demonstrated a one parameter, and a two parameter Level 2 tuning of blended encoding algorithms. In Ref. 15 Yang *et al.* performed a Level 3 design which attempts to maximize the diffraction efficiency of $\mathbf{a}_c(x)$ by three different search/optimization procedures, followed by a single encoding. The problem is partitioned into separate, non-interacting modules. There is no feedback of the resulting intensity $I(f)$ to fine tune $\mathbf{a}_c(x)$ or the encoding algorithm. These procedures require no evaluations by IFFT. Jared and Ennis used a descent search method similar to the Newton-Raphson method to iteratively correct for changes in the peak intensities of autocorrelations due to the SLM modulation characteristics [17].

Vangular observed that this procedure can be directly adapted to improving the uniformity of the intensity patterns from spot array generators [20]. This method corresponds to the feedback of $I(f)$ as indicated by the blue dotted path in Fig. 1a.

4. Illustrative Scanning Sequences

To this point we have presented our conception of a real-time diffractive scanner/illuminator. We have focused on speed limitations due both to framing time of SLM's and computational rate for on-line design systems. These discussions are intended to provide a perspective from which one can appreciate the use of SLM's as real-time scanners. In order to complete this picture we demonstrate unique possibilities for scanning with diffractive SLM's through the presentation of experimentally recorded, live video sequences of the far-field patterns from a phase-only SLM. Specific issues and considerations in using SLM's in this way are brought out by these demonstrations, including opportunities in certain situations for computational speedups.

The demonstrations all are performed with a 120 x 128 pixel (the 8 outermost columns of the device are inoperative), reflective SLM from Boulder Nonlinear Systems, Inc. (BNS). The cell is filled with nematic, parallel aligned liquid crystal. The laser polarization is linear and aligned to a collimated green laser beam (532 nm) to produce phase-only modulation of up to 2π . A lens placed one focal length from a CCD video camera forms a Fourier transform on the imaging area of the camera. Unless otherwise noted, the image of the diffraction pattern covers approximately the entire area between the on-axis (0,0) diffraction order and the (1,1) diffraction order (corresponding to the reciprocal of the pixel spacing). This region of the diffraction plane has 120 x 128 resolution cells or a SBWP of 15,360. There is always a very bright spot on the optical axis which is due to Fresnel reflections from the cover glass and optical losses in the modulating layer [9]. Aside from the on-axis spot the device performs very similar to an ideal phase-only SLM. One other feature of the SLM is the subaperture that defines a pixel. This leads to a sinc^2 intensity rolloff along horizontal and vertical axes of the diffraction plane, and a sinc^4 along the diagonal. In some of the diffraction patterns this rolloff is compensated in the design. Additional details of the experimental apparatus have been reported in Ref. 9.

At this time no complete on-line design system exists. The modulation patterns typically are designed off-line and then loaded in sequence onto the SLM. In some cases, when only Level 1 design is adequate, the patterns are designed and loaded as created. Using a 100 MHz Pentium computer and a C++ program this takes around 0.5 second per frame to compose and encode a 10 spot function. However, no efforts have been taken to optimize the numerical calculations. Specifically we found that the computation time of a 128 x 128 FFT is about 4X faster than the time used to compose the 10 spot functions. This speed advantage is attributed to the FFT implementation using precomputed values of the complex exponential. However, the purpose of this section, rather than demonstrating speed, is to illustrate various scanning functions and to suggest their usefulness.

Arbitrary scanning. Fig. 2a shows a sequence of five diffraction patterns composed of 63 to 73 spots. The movie shows a repeating sequence of the five images. This illustrates the ability of the SLM to generate rather arbitrary images. Fig. 2b shows the entire area of the image that was captured by the CCD camera. This is nearly the entire diffraction plane between the (0,0) and (1,1) orders. The modulation patterns were designed by the IFTA (see Fig. 1b) followed by MD-PRE of the resulting complex valued function $\mathbf{a}_+(x)$. The performance of the theoretical design for this movie (as well as for all the movies in this paper) is reported in Table 1. It is interesting to compare the performance with $\mathbf{a}(x)$, the traditional IFTA design [which can be interpreted as MDE of $\mathbf{a}_+(x)$.] While IFTA followed by MD-PRE results in a lower diffraction efficiency than traditional IFTA (73 % to 82 %), it has improved fidelity as measured by signal-to-peak ratio (SPR, 12 to 3.5) and nonuniformity (NU, 19 % to 32 %). Using MD-PRE instead of MDE after IFTA, produces a faint background speckle pattern across the entire SBWP (instead of isolated, but more intense noise peaks.) Consequently, even though MDE has a higher signal-to-noise ratio

(SNR) than MD-PRE (720 to 429), the lower average noise of MD-PRE, as measured by SPR, represents the more faithful rendition of the desired diffraction pattern – especially for applications that use the full SBWP of the SLM. These relationships between metrics have been reported in detail our papers listed in *References and links*.

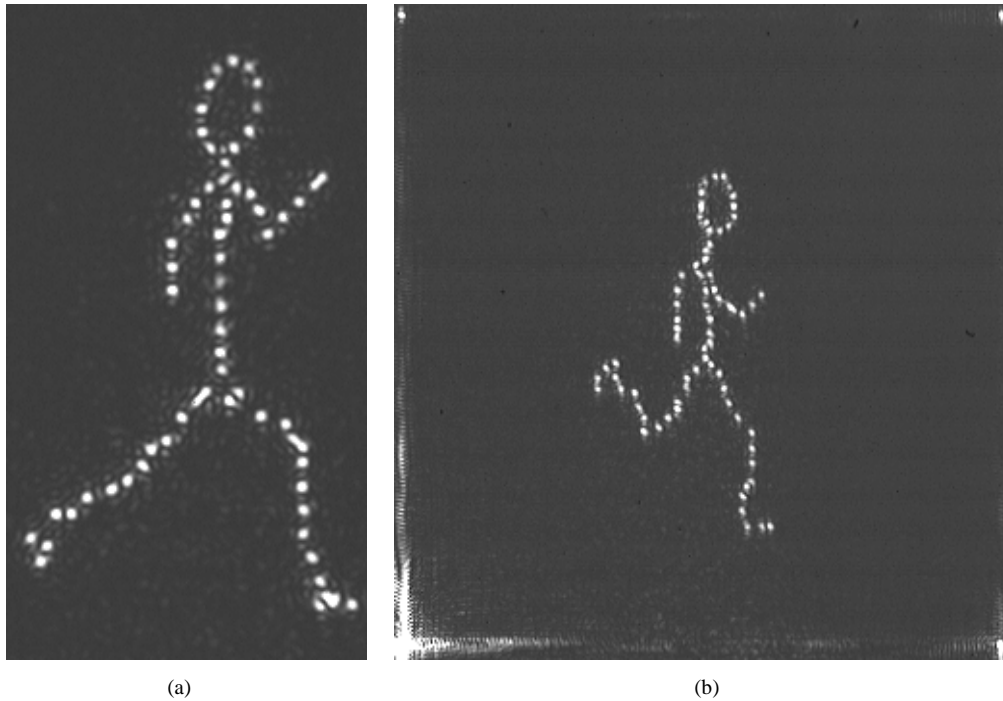


Fig. 2. (a) (1.62 MB) Movie of arbitrary scanning by SLM, (b) image with (0,0) to (1,1) orders indicated

Table 1. Information on diffraction pattern images, design method and theoretical performance

Figure	Width (%)	Complex function composed by	Encoding method	η (%)	NU (%)	SPR	SNR
Fig. 2	44	IFTA (Fig. 1b)	MD-PRE of $\mathbf{a}_x(x)$	73	19	12	429
Fig. 3a	95	all $\phi_i=0$	MD-PRE, $\gamma=1$	9	12	4	324
Fig. 3b	95	same as Fig. 3a	MD-PRE, $\gamma=\infty$	11	9	3	404
Fig. 4	95	Based on max. η 1x7 array [9]	MD-PRE, $\gamma=1.4$	74	6	72	975
Fig. 5a	55	random ϕ_i , continuous f_i	MD-PRE, $\gamma=1.2$	38	10	13	1004
Fig. 5b	55	random ϕ_i , discrete f_i	MD-PRE, $\gamma=1.2$	38	10	13	1004
Fig. 6a	100	periodic spatial interleaving	none	100	0	∞	∞
Fig. 6b	100	random spatial interleaving	none	8	17	2	89
Fig. 7a	87	aperture subdivision	MD-PRE, $\gamma=1.5$	61	–	–	–
Fig. 7b	87	superposition and subdivision	MD-PRE, $\gamma=1.5$	54	–	–	–
Fig. 8a	46	Select ϕ_i randomly	MD-PRE, $\gamma=1.3$	25	9	12	111

Theoretical performance: Measured from 128 x 128 FFT of designed function for one selected movie frame.

Width: Width of movie image in x as relative to SBWP in x (i.e. grating frequency). Most images are square.

η : Diffraction efficiency – Ratio of energy at the desired frequencies to energy in the entire diffraction pattern.

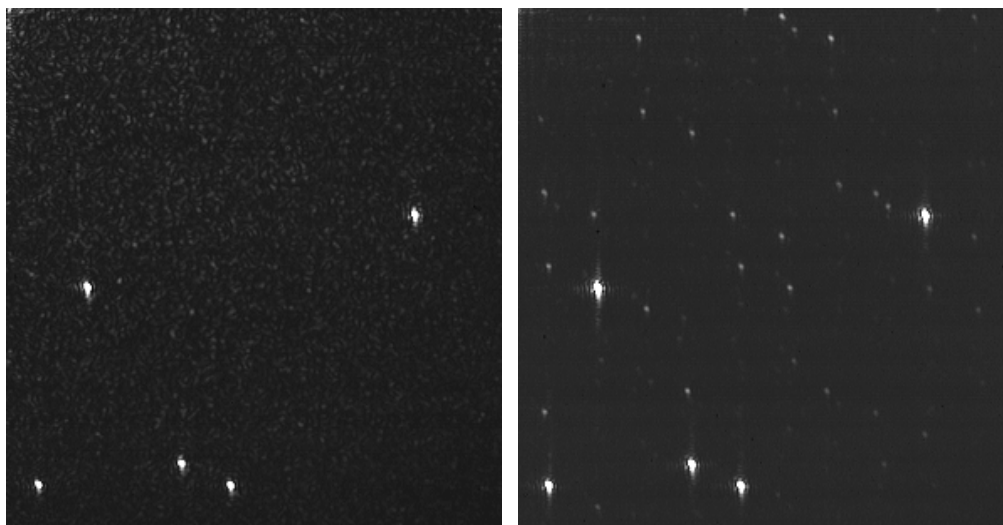
NU: Nonuniformity – Standard deviation of the intensity of the spot array relative to the average spot intensity.

SPR: Signal-to-peak-ratio – Average intensity of the spots relative to intensity of the largest noise sidelobe.

SNR: Signal-to-noise-ratio – Average intensity of the spots relative to the average background noise.

Reduction of sidelobes. The problems with noise sidelobes can be better appreciated by comparing the result of encoding the same desired functions by two different encoding algorithms. The particular scanning sequence has five spots moving on five different trajectories. Fig. 3a is the result for MD-PRE and Fig. 3b is the result for using MDE. MDE maps the desired function the closest distance to the available modulator values. This results in a minimum mean squared

error design. However, this systematic method of mapping produces distinct sum and difference frequencies (akin to a hard limiter in communications.) The sidelobes in Fig. 3b are much more intense, and thus, easier to falsely classify as desired signal than the background speckle in Fig. 3a.



(a)

(b)

Fig. 3a. Movies of sidelobe generation by (a) MD-PRE (2.41 MB) and by (b) MDE (2.41 MB)

Pattern translation. In some cases it may be desirable to scan a desired pattern to several locations as illustrated in Fig. 4. With a continuous phase, phase-only SLM, scanning of a desired function can be particularly efficient. The computation involves addition of the desired function to a phase ramp, followed by modding the phase, as needed, back into a 2π phase range. Thus while the Fig. 4 image requires the addition of 49 functions to compose the desired modulation, the position can be changed by adding a single function to the encoded function. Note that the design of the desired complex function is based on published maximum diffraction efficiency designs for one dimensional arrays of spots [1]. A numerically efficient method of function composition [$O(N)$ multiplies] is used to compute the one dimension modulation and then form the outer product of the modulation with itself.

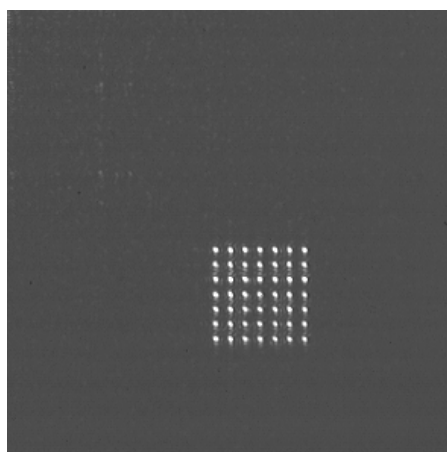


Fig. 4. (1.91 MB) Movie of translation of a fixed pattern.

Continuous scanning. The examples presented so far do not demonstrate continuous scanning. Fig. 5a and the corresponding movie show scanning at various rates from x to y diffraction limited spots diameters per frame. Fig. 5a specifically shows the sum of the multiple frames in the movie. The line rotates 2° per frame and the spots are separated by 6 diffraction limited spot diameters. The fifth line from the pivot point in Fig. 5a corresponds to approximately a one pixel per frame rotation rate. Lines of this radius or less should (and do) appear continuous and lines at greater radii should appear as discrete samples. For the sixth and seventh lines there is still some overlap between the individual spots, which is due to camera saturation and contrast adjustments to the published image. The desired function is composed by addition of complex sinusoids of arbitrary frequencies. A second method of composition is to use the IFFT. Fig. 5b illustrates the result of using a 128×128 point IFFT to synthesize a spot pattern. As opposed to Fig. 5a, in Fig. 5b the spots only form at the discrete frequencies corresponding to the frequency sample points of the IFFT. Continuous scanning can be approached by increasing the number of sample points in the IFFT, but at an increasing computational cost. In some cases smaller IFFT's could be used, as well. If the desired modulation is periodic, then one period of the function can be calculated followed by copying or repeating the function to the full size of the SLM. This would be possible for the function used to produce the 7×7 spot array in Fig. 4, which consists of a 4×4 array of unit cells.

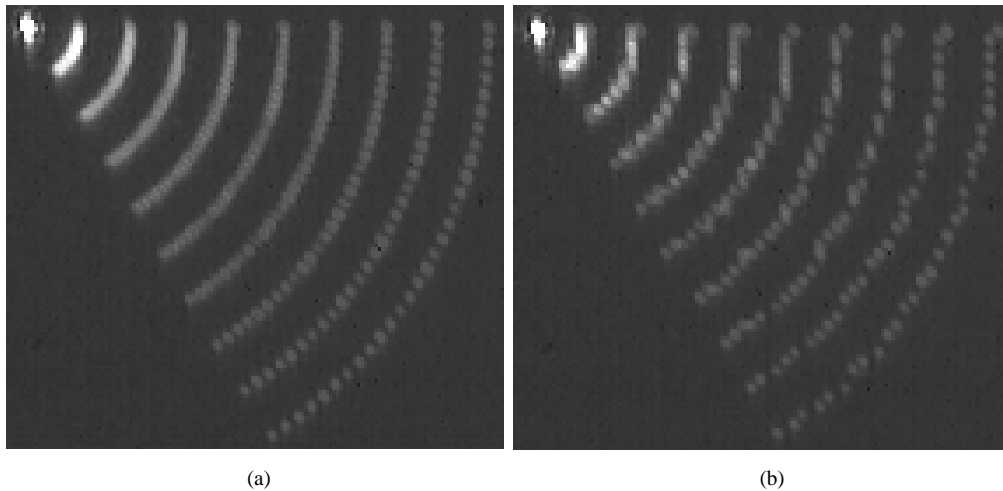


Fig. 5. Movies of continuous scanning (a) by composition (579 KB) and (b) by 128×128 IFFT (611 KB). The fixed images in this figure are the summations of the images from the entire sequence.

Replicated scans in parallel. One useful scanning arrangement is to scan the same pattern over multiple fields in parallel. This can be accomplished by under-sampling the SLM, which produces replicas over the full SBWP of the diffraction plane. An example of this is shown in Fig. 6a. Here a sample of the desired function is programmed every fourth pixel in x and y . In this example 16 linear phase ramps are spatially multiplexed to produce 16 spots replicated into 16 regions. Because each elementary function is phase-only and spatially orthogonal this modulation function has a theoretical diffraction efficiency of 100%. With 256 spots the entire 120×128 SBWP of the diffraction plane could be systematically scanned in 60 frames. This corresponds to an equivalent raster scan rate (using a single spot scanner) that is twice the SLM frame rate.

A simple way to produce a nearly identical pattern without replications is to randomly sample, rather than regularly sample the desired function. This method was originally reported by Davis and Cottrell [21]. The method does generate speckle. An example of this design method is presented in Fig. 6b. A speckle pattern background is produced as a result of the random spatial multiplexing of the multiple functions. Also the intensity of individual spots can be adjusted by

increasing or decreasing the percentage of the time that the corresponding modulation function is sampled.

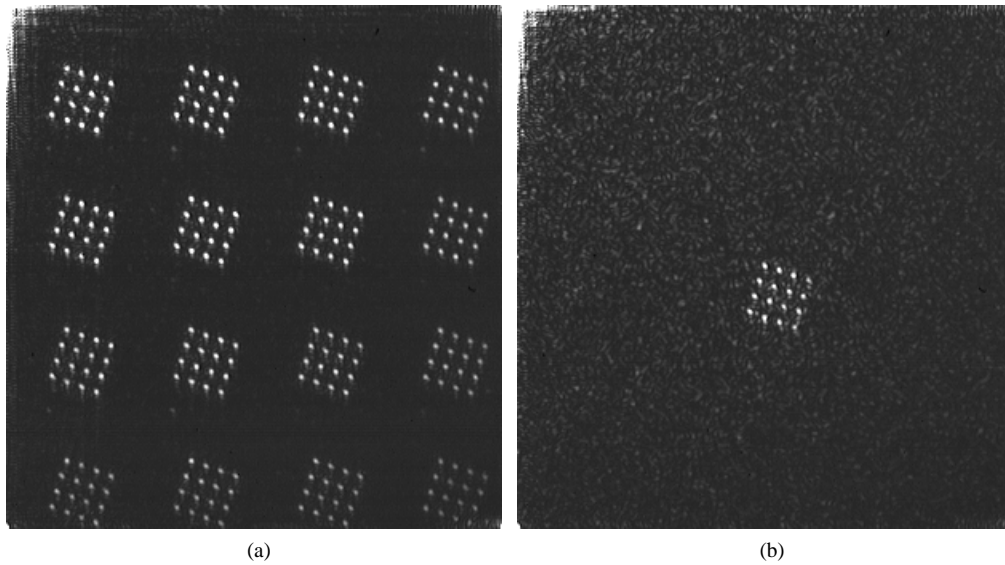


Fig. 6. Movie of (a) parallel replicated scanning by periodic sampling (2.13 MB) and (b) by non-replicated scanning by random sampling (2.23 MB) of the elementary functions.

Variable resolution scanning. Another method of increasing scanning speed (mentioned in Sec. 2) is to design spots that have greater widths than the diffraction limited spot width of the SLM aperture. For the result shown in Fig. 7a, the desired modulation plane function is divided into 9 square regions (32 x 32 pixels each), 2 rectangular regions (60 x 32 pixels) and 1 rectangular region (24 x 96 pixels). Each region is filled with a circular or elliptical aperture function of unity transmittance. The surrounding region of zero transmittance is encoded by MD-PRE. The resulting Airy diffraction patterns are desirable because the first diffraction ring is considerably lower in intensity than the sidelobe of sinc^2 patterns. In Fig. 7b a second layer of

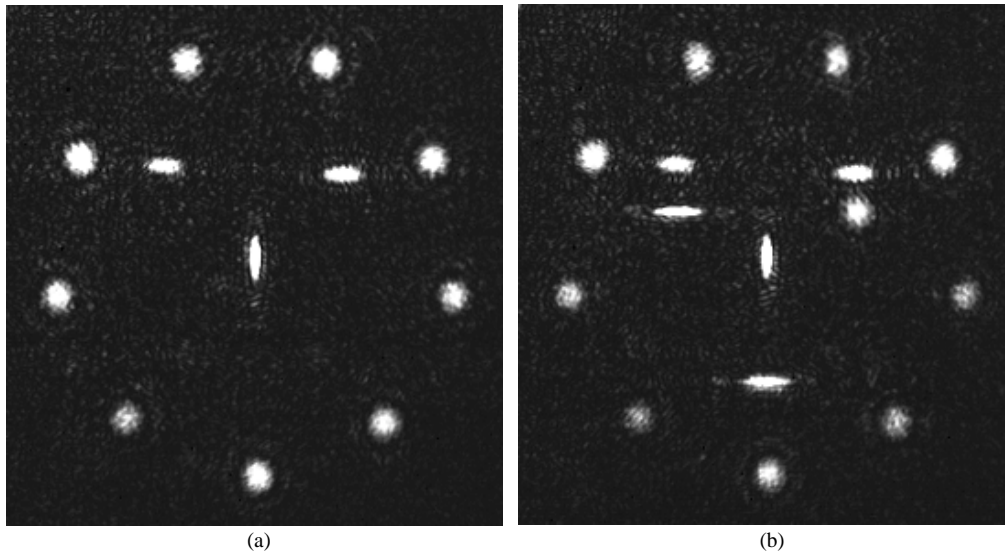


Fig. 7. Movie of multiple widened spots (a) by parallel division of the SLM into multiple SLM's (578 KB) and (b) by adding two sets or layers of spatially multiplexed functions together (1.12 MB.)

elliptically windowed functions is added to the first layer of functions to produce the three additional spots. Two of the bounding rectangles are 120 x 20 pixels and one is 30 x 30 pixels.

Time-averaged scanning. Statistically based encoding algorithms [9-13] necessarily produce noise which is manifested as deviations of the actual diffraction pattern intensities from the desired intensities and speckle background. As seen in Figs. 3-7, these noise effects can be kept to manageable levels for many practical designs. However, these effects can be reduced further by ensemble averaging. Specifically, statistical encoding algorithms produce the desired intensity pattern on-average plus a background that corresponds to the average speckle intensity [12]. Multiple realizations are produced by performing repeated encodings of the desired modulation function. For each encoding a unique random sequence is used. The resulting diffraction plane intensity patterns are averaged together. An experimental demonstration of this procedure for an encoding of an apodized aperture is presented in Ref. 12. Fig. 8 illustrates the improvement in performance of the 7 x 7 spot array design of Fig. 4 for 50 realizations used in the average. The computational load is $O[N]$ function calculations for each encoding and $O[N]$ additions to add the new intensity pattern to the ensemble. Therefore, if the pattern is not changing over multiple cycles, then a time-averaging procedure can be used to produce a more accurate realization of the desired diffraction pattern, with minimal increase in the computational requirements.

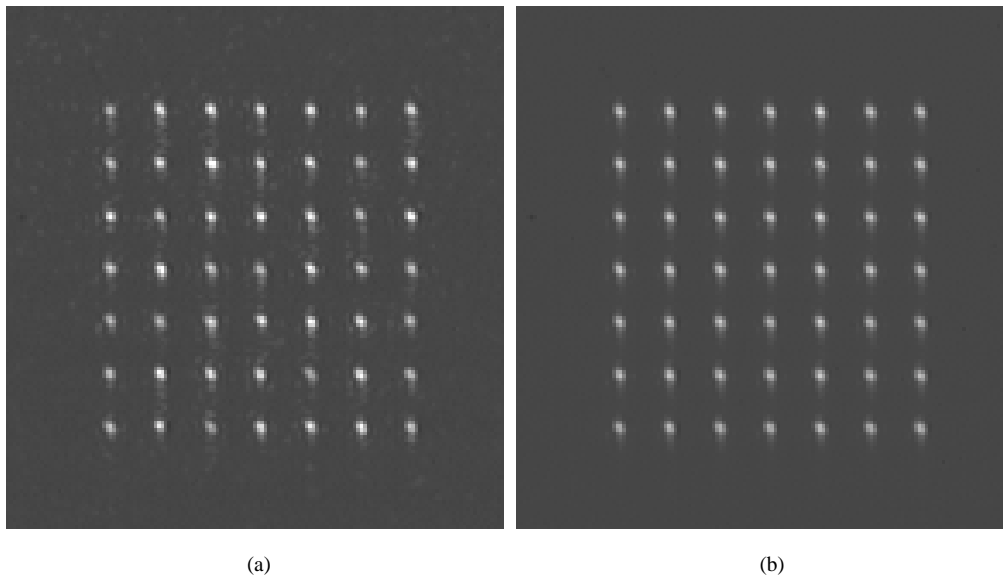


Fig. 8. Image of (a) individual realizations of the spot array (337 KB) and (b) average result of 50 individual realizations of the spot array.

Broad area scene illumination. Modulation patterns can be specified that uniformly illuminate the diffraction plane. As pointed out in Section 1, there is no energy advantage to using diffractive SLM's for this purpose. However, the addition of a broad illumination capability to a multi-spot pattern generator could prove useful for adaptive tracking and designation of objects. While, it should be possible to designate objects and update their positions based on changes in the intensity of the spots reflected from objects, a broad area search is required initially to identify the objects of interest. Using the SLM to illuminate the scene reduces the amount of hardware needed, since a single video camera can be used to observe the entire scene and to monitor the intensity of laser spots reflected from the objects in the scene. Laser illumination is not only required for use in the dark, but it also is useful for lighted scenes. In lighted environment, a narrowband color filter would be placed over the camera to remove other contributions of light and to maximize the detectability of the laser returns. In some situations the laser illumination

even can be weak enough to go unnoticed by an observer in the scene.

To produce broad area illumination we programmed the SLM with a sequence of random phases that are uniformly distributed between 0 and 2π . This diffuser produces a speckle pattern at the Fourier transform plane on a copper coin. The coin is illuminated and imaged at $\sim 20^\circ$ from vertical (Fig. 9a.) The illumination quality can be brought closer to that of incoherent light by averaging multiple realizations of the diffuser. Fig. 9b shows the average image for illumination with 50 statistically independent diffusers.

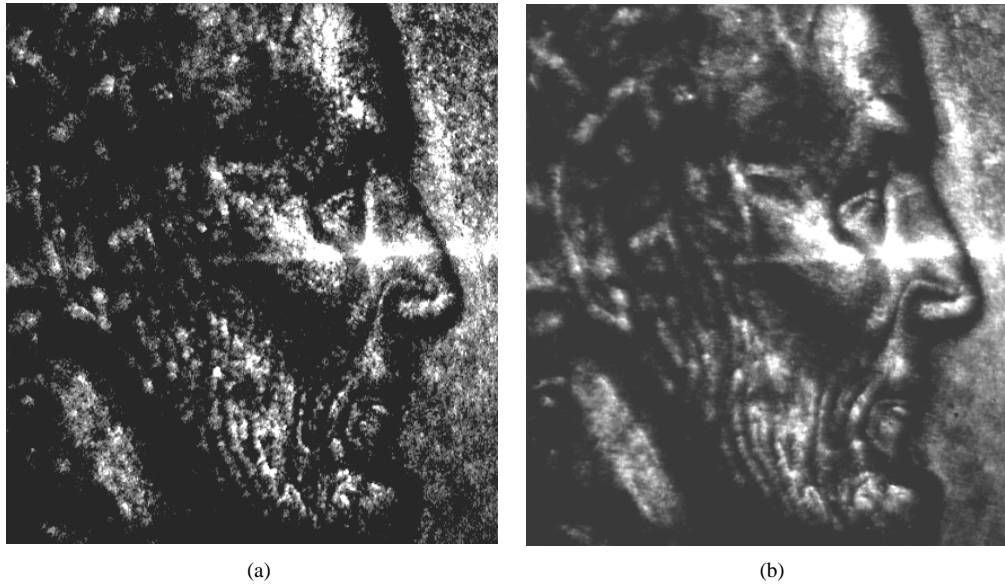


Fig. 9. Image of (a) individual realization of a speckle-illuminated coin and (b) average result of 50 individual realizations of the speckle-illuminated coin.

5. Summary and Conclusion

Using a frame-addressed SLM in a Fourier transform arrangement provides a variety of intensity patterns that may provide much more general scanning capabilities than is possible with traditional inertial type scanners. This increased flexibility comes at a cost of an increased computational load. However, if the system is used as part of a multi-object tracking system or in a vision-guided robotic navigation system, then the computational load associated with on-line design of the diffraction patterns may be commensurate with the loads associated with image processing and supervision of the entire system. In light of the available response time of an adaptive system, a general approach to on-line diffraction pattern has been presented that emphasizes producing designs of increasing fidelity as more computation time is available. The general approach requires iterative optimization or global search if adequate time is available. However, specialized modulation patterns can be devised using spatial multiplexing (as in Figs. 6 and 7) that do not require either optimization or encoding. Other situations can be exploited for speedups, such as translating an identical pattern (in Fig. 4) or imposing special structure on the desired function (e.g. rectangular separability in the design of the spot array in Fig. 4 [13]). Many other possibilities might be exploited by taking into account the scene environment (e.g. spatial extent, velocity and number of objects in the scene.)

Based on the above considerations we believe that affordable scanning systems could be developed that run at practically useful rates. These systems could provide powerful advantages to advanced and intelligent military and commercial systems. The SLM scanners could be used to convert a single laser target designator into a multi-target designator. It could be applied to long range designation of objects in outer space, to shorter range designation on the battlefield,

and to close-in weapons defense of naval vessels. For autonomous control a vision system with multi-object tracking is needed to steer, point and adapt the laser spots. A commercial application of the same system is to coordinate the activities of several distributed robotic package handlers. Lasers used to highlight the packages would make their motion easier to track with machine vision. A laser pattern generator and vision system mounted on a mobile robot could support feature-based navigation. The further development of a diffractive SLM based scanner would be interesting and challenging in terms of algorithm refinement and integration.

Acknowledgments

The funding for this study was from National Aeronautics and Space Administration cooperative agreement NCC5-222, Office of Naval Research grant N00014-96-1-1296, and Ballistic Missile Defense Organization (through Air Force Research Laboratory) grant F19628-99-C-0084.